



Article

Isolation and Polyphasic Characterization of *Desulfuromonas versatilis* sp. Nov., an Electrogenic Bacteria Capable of Versatile Metabolism Isolated from a Graphene Oxide-Reducing Enrichment Culture

Li Xie ^{1,†} , Naoko Yoshida ^{1,*,†} , Shun'ichi Ishii ² and Lingyu Meng ¹

- ¹ Department of Civil Engineering, Nagoya Institute of Technology (Nitech), Nagoya 466-8555, Aichi, Japan; xie705049124@126.com (L.X.); meng.lingyu@nitech.ac.jp (L.M.)
- ² Institute for Extra-Cutting-Edge Science and Technology Avant-Garde Research (X-Star), Japan Agency for Marine-Earth Science and Technology (JAMSTEC), Yokosuka 237-0061, Kanagawa, Japan; sishii@jamstec.go.jp
- * Correspondence: yoshida.naoko@nitech.ac.jp; Tel.: +81-527-355-437
- † These authors have contributed equally to this work and share first authorship.

Abstract: In this study, a novel electrogenic bacterium denoted as strain NIT-T3 of the genus *Desulfuromonas* was isolated from a graphene-oxide-reducing enrichment culture that was originally obtained from a mixture of seawater and coastal sand. Strain NIT-T3 utilized hydrogen and various organic acids as electron donors and exhibited respiration using electrodes, ferric iron, nitrate, and elemental sulfur. The strain contained C16:1 ω 7c, C16:0, and C15:0 as major fatty acids and MK-8, 9, and 7 as the major respiratory quinones. Strain NIT-T3 contained four 16S rRNA genes and showed 95.7% similarity to *Desulfuromonas michiganensis* BB1^T, the closest relative. The genome was 4.7 Mbp in size and encoded 76 putative *c*-type cytochromes, which included 6 unique *c*-type cytochromes (<40% identity) compared to those in the database. Based on the physiological and genetic uniqueness, and wide metabolic capability, strain NIT-T3 is proposed as a type strain of '*Desulfuromonas versatilis*' sp. nov.

Keywords: *Desulfuromonas*; electrogenic bacteria; nitrate respiration; graphene oxide



Citation: Xie, L.; Yoshida, N.; Ishii, S.; Meng, L. Isolation and Polyphasic Characterization of *Desulfuromonas versatilis* sp. Nov., an Electrogenic Bacteria Capable of Versatile Metabolism Isolated from a Graphene Oxide-Reducing Enrichment Culture. *Microorganisms* **2021**, *9*, 1953. <https://doi.org/10.3390/microorganisms9091953>

Academic Editors: Annette Rowe and Akihiro Okamoto

Received: 10 July 2021
Accepted: 9 September 2021
Published: 14 September 2021

Publisher's Note: MDPI stays neutral with regard to jurisdictional claims in published maps and institutional affiliations.



Copyright: © 2021 by the authors. Licensee MDPI, Basel, Switzerland. This article is an open access article distributed under the terms and conditions of the Creative Commons Attribution (CC BY) license (<https://creativecommons.org/licenses/by/4.0/>).

1. Introduction

Anaerobic and extracellular electron-transferring (EET) bacteria are ubiquitously involved in the redox flow via solid conductors. *Geobacter* and *Shewanella* have been extensively studied for their functional roles in terrestrial and marine subsurface, whose anoxic environments are deficient in soluble electron acceptors. The unique metabolism of such bacteria has been applied in bioelectrochemical systems (BESs) to be used for wastewater treatment [1], production of renewable energy and value-added products [2], and bioremediation [3]. Both culture-dependent and -independent studies have revealed the presence and functional role of electrogenic microbes other than *Geobacter* and *Shewanella* [4]. Various factors, such as availability of the electron donor [5], the electric potential of a solid conductor [6], and the origin, affect the microbial composition in the system. Additionally, the surface chemistry of electrodes provides selective pressure during the early growth of the biofilm [7].

The genus *Desulfuromonas* has received much attention as a common electrogenic bacteria present in BESs [8–10]. *Desulfuromonas* species are found in natural environments, such as aquifers [11], sediment cores [12], and terrestrial mud volcanoes [13], suggesting a wide distribution. The genus *Desulfuromonas* consists of anaerobic chemoheterotrophs and was first proposed after the isolation of an elemental sulfur-reducing bacterium, *Desulfuromonas acetoxidans* DSM 684^T, from anaerobic sulfide-containing marine

mud [14]. At present, *D. acetoxidans* DSM 684^T and seven other valid species have been proposed. *D. acetexigens* 2873^T [15], *Desulfuromonas palmitatis* SDBY1^T [16], *Desulfuromonas thio-phila* NZ27^T [17], *Desulfuromonas chloroethenica* TT4B^T [18], *Desulfuromonas michiganensis* BB1^T [19], *Desulfuromonas svalbardensis* 112^T [20], and *Desulfuromonas carbonis* ICBM^T [21] have been isolated from anoxic freshwater sediments, marine sediment, freshwater mud, freshwater sediment, pristine river sediment, Arctic marine sediments, and coal-bed water, respectively. Recently, additional strains including *Desulfuromonas* sp. TF [22], *Desulfuromonas* sp. AOP6 [23], *Desulfuromonas* sp. TZ1 [24], and ‘*Desulfuromonas soudanensis*’ WTL [25] have been isolated from tidal flat sediment, sub-seafloor sediment, marine sediments, and anoxic deep subsurface brine, respectively.

All valid species of *Desulfuromonas* grow anaerobically and reduce sulfur, and exhibit iron respiration coupled with acetate oxidation; however, they are unable to respire using soluble nitrogenous and sulfuric compounds. The respiration specific to solid minerals and the presence of *Desulfuromonas* species in BESs suggest the substantial involvement of *Desulfuromonas* in electrode-driven metabolism, although such activity has been rarely proven in pure cultures. None of the valid species, except for two strains including *Desulfuromonas* sp. TZ1 [24] and ‘*D. soudanensis*’ WTL [25], generate an electric current in pure cultures, and both have been isolated from electrodes set up in environments, such as marine sediment and Soudan mine, respectively. These results suggest that *Desulfuromonas* species play substantial roles similar to those of two representative electrogenic genera, *Geobacter* and *Shewanella*, in microbial elemental cycling on solid conductors, especially in marine sediments.

Presently, the genomes of two strains, *D. soudanensis* WTL [25] and *Desulfuromonas* sp. AOP6 [23], have been published, and the genome of another strain, DDH964, is unpublished but uploaded on the National Center for Biotechnology Information (NCBI) database under the accession number CPO15080. The genomes are 1.64–4.40 Mb in size, contain 37.9–65.9% of broad G + C content, and have 2181–3924 coding sequences (CDSs). All three genomes encode a complete TCA cycle, a non-oxidative pentose phosphate pathway, Embden-Meyerhof-Parnas glycolysis/gluconeogenesis, and abundant CDSs associated with *c*-type cytochrome biosynthesis. The number of putative multiheme *c*-type cytochromes ranges from 37–44, and the number is comparable to those in the genera *Geobacter* and *Shewanella*. Additionally, genes involved in the biosynthesis of type IV pili, known to be involved in the formation of conductive biofilm [26], are commonly present in the three genomes.

In this study, a novel electrogenic bacterium of the genus *Desulfuromonas*, ‘*Desulfuromonas versatilis*’ NIT-T3 was isolated from an enrichment culture of graphene oxide-reducing bacteria (GORB) that were initially obtained from a mixture of seawater and coastal sand [27]. GORB have been applied in the formation of hydrogel electrodes that generate electricity using synthetic medium [28], soil [29], and wastewater [30–32]. Physiological and genomic analysis of strain NIT-T3 revealed versatile metabolism, and the findings expand the understanding of the metabolism in the genus *Desulfuromonas* and its ecology in natural and artificial environments.

2. Materials and Methods

2.1. Isolation and Growth Conditions

Strain NIT-T3 was isolated from an enrichment culture of GORB (CS culture) that was obtained from a mixture of seawater and coastal sand, as described previously [27]. A DS-basal medium used for the isolation and growth of the strain contains 20 g/L NaCl, 0.3 g/L KCl, 0.5 g/L NH₄Cl, 0.1 g/L CaCl₂·2H₂O, 4 g/L MgCl₂·6H₂O, 0.6 g/L KH₂PO₄, 2.5 g/L NaHCO₃, 1 mL/L SL-10, 1 mL/L Se/W solution, vitamin-solution, and 0.2 mg/L resazurin and the basal medium was prepared anaerobically under flashing N₂:CO₂ (80:20, *v/v*) [28]. The strain NIT-T3 was isolated from an anaerobic DS-AQDS agar plate which DS-basal medium supplemented with 10 mM acetate, 5.0 mM anthraquinone-2,6-disulfonate (AQDS), 1 mM Na₂SO₄, and 1.5% agarose. After 7–14 d of incubation at

28 °C, electrochemically active colonies showed orange halos, which was the color of the reduced form of AQDS. The colony culture was then purified via repeated agar-shake cultivation using DS-AF agar plate, DS-basal medium supplemented with 10 mM acetate, 0.1% yeast extract, 1.5 mM Na₂S, 5.0 mM fumarate, and 1.5% agarose. The purified culture was then phylogenetically identified based on the 16S rRNA gene sequence amplified from the cell lysate [33] and named strain NIT-T3. Strain NIT-T3 was routinely cultured using the liquid DS-AF medium. In total, 7–14 d of anaerobic cultivation at 28 °C was sufficient to achieve full growth.

2.2. Morphological, Physiological, and Biochemical Analyses

The morphology of strain NIT-T3 was evaluated using field-emission scanning electron microscopy (JSM-7800F; JEOL Ltd., Tokyo, Japan) operating at 1.0 kV; spore-forming ability and Gram staining nature were determined via optical microscopy, as described previously [34]. Motility was determined using the hanging drop method [34]. The effect of NaCl on cell activity was evaluated by monitoring growth in DS-AF medium supplemented with 0–8.0% (*w/v*) NaCl. The effect of pH was also determined using a bicarbonate-free medium adjusted to a pH ranging from 4.8 to 8.4 using sodium bicarbonate and by adjusting the CO₂ concentration in the headspace gas. Temperatures ranging from 4 °C to 40 °C with approximate intervals of 5 °C were applied to determine the effect on cell growth.

Formate, acetate, butyrate, lactate, pyruvate, succinate, malate, isopropanol, glucose, glycerol, isobutyrate, caproate, benzoate, phenol, methanol, ethanol, butanol, and fructose at 10 mM, and 0.5 g/L peptone and yeast extract were tested as potential electron donors during nitrate reduction. Potential electron acceptors were evaluated by observing growth and detecting the oxidation of 5.0 mM acetate in the presence of 10 mM fumarate, 5 mM nitrate, 10 mM sulfate, 10 mM thiosulfate, 5.0 mM AQDS, and 10 mM malate. Production of electric current by the strain NIT-T3 was evaluated via electrochemical cultivation using a graphite plate inoculated with NIT-T3, as described previously [35].

2.3. Chemotaxonomic Analysis

The cellular fatty acid composition and isoprenoid quinones present in NIT-T3 were investigated by Techno Suruga Laboratory Co., Ltd. (Shizuoka, Japan). Isoprenoid quinones were extracted, as described by Tamaoka et al. [36]. Cellular fatty acids were analyzed using cells cultured in liquid DS-AF medium at 28 °C for 14 d. The fatty acid profile was analyzed using the Sherlock Microbial Identification System version 6.0 (MIDI) using the TSBA6 database.

2.4. Genetic Characterization

Genomic DNA was extracted from strain NIT-T3, as described previously [37]. Sequencing was performed using a combination of the Illumina Miseq and Nanopore MinION. In total, 1.8 M reads (1.02 Gbp) of Illumina paired-end reads (150 × 2) and 0.37 M Nanopore reads (1.76 Gbp) were subjected to error removal using Short Read Manager and assembled using Unicycler-0.4.7. The complete genome of NIT-T3 was successfully determined, and gene prediction and genome annotation were performed using DFAST [38]. Comparison of the genes between NIT-T3 and other *Desulfuromonas* species was based on bidirectional best hits at 40% identity and 80% query coverage using SEED Viewer version 2.0 [39] and basic local alignment search tool in the NCBI database. The sequence of the NIT-T3 genome was deposited in the DNA Databank of Japan/GenBank under the accession number AP024355.

The 16S rRNA gene sequences from all publicly available *Desulfuromonas*, *Desulfuromusa*, *Geobacter*, *Geopsychrobacter*, and *Pelobacter* genomes were downloaded from NCBI. A phylogenetic tree based on 16S rRNA gene sequences of NIT-T3 and other members of the family *Desulfuromonadaceae* was generated using MEGA X based on the neighbor-joining method [40].

3. Results

3.1. Isolation of NIT-T3

Anaerobic cultivation of AQDS-supplemented agar plates inoculated with the TGOA enrichment culture resulted in the formation of colonies that showed a change in color from colorless to orange. This suggested the ability of the colony to reduce AQDS and utilize it as an extracellular electron acceptor. A single colony was picked from the agar culture, purified via repeated agar-shake cultivation, and then re-cultivated in liquid DS-SF medium. Finally, based on the uniformity in microscopic morphology and 16S rRNA gene sequences, a liquid culture was selected and further purified by repeating the agar cultivation step. Cells of strain NIT-T3 were Gram-negative, non-spore-forming, rod-shaped, and approximately 0.5 μm in width and 1.5 μm in length (Figure 1A).

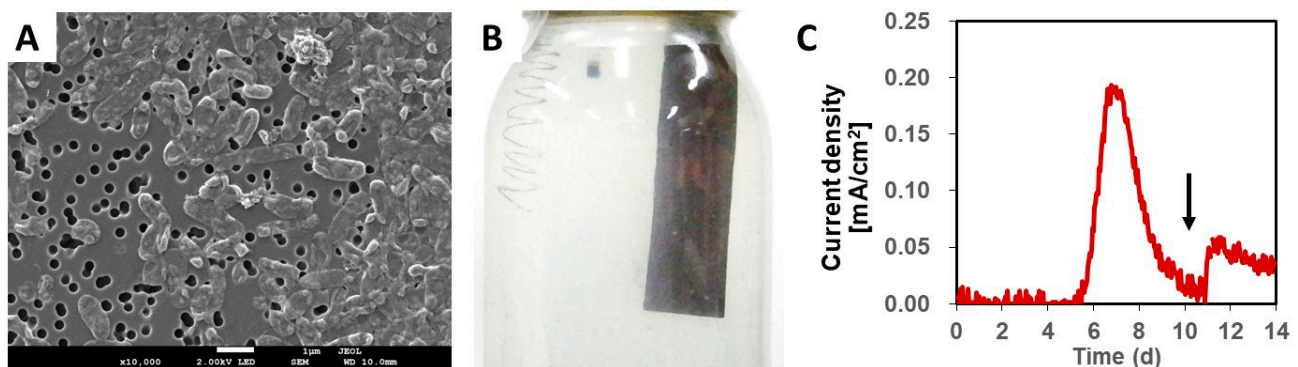


Figure 1. Morphology and electrogenic properties of strain NIT-T3. (A) Scanning electron microscopic image of strain NIT-T3. The white bar indicates 1 μm of length. (B) Growth of a biofilm on an electrode in an electrochemical culture. (C) Electric current production by strain NIT-T3. The arrow in panel C indicates a spike of acetate addition.

The strain NIT-T3 produced an electric current on a graphite electrode in the presence of acetate and simultaneously generated a thin biofilm on the electrode surface (Figure 1B). The current in the electrochemical cultivation medium was rapidly generated and the maximum level was detected in the range of 0.18 to 0.19 mA/cm^2 on days 6 and 7 (Figure 1C). Electric current production decreased gradually with time; however, it increased immediately after adding acetate to the media. These results indicated that strain NIT-T3 grows by coupling EET to electrode with acetate-oxidation.

3.2. Phylogenetic Identification Based on 16S rRNA Sequencing

Strain NIT-T3 was found to contain four 16S rRNA operons (*rrn1-4*); one of them showed 95.5–95.8% similarity to the three *Desulfuromonas* strains. The copy number was higher than that in *Desulfuromonas* strains containing two copies, and equal to that in four *Geobacter* and two *Pelobacter* strains: *G. bemidjiensis*, *G. bremensis*, *P. acetylenicus*, and *P. propionicus*. The 16S rRNA gene-based phylogenetic tree revealed that all four *rrns* formed a cluster with sequences of five strains of the genus *Desulfuromonas* of the family *Desulfuromonadaceae* (Figure 2).

Strain NIT-T3 showed only 95.7% closest similarity based on 16S rRNA gene sequences to that of *D. michiganensis* BB1^T. Similarities with seven other species of the genus *Desulfuromonas* ranged from 92.9% to 95.4%. The 16S rRNA gene sequence similarity of strain NIT-T3 to members of the genera *Pelobacter*, *Desulfuromusa*, and *Geobacter* were 89.7–94.9%, 90.7–90.9%, and 90.6–91.6%, respectively. According to the cut-off values of 98.2–99.0% [41], and 98.65% similarity among single species [42], the strain NIT-T3 may be proposed as a strain of a novel species of the genus *Desulfuromonas*.

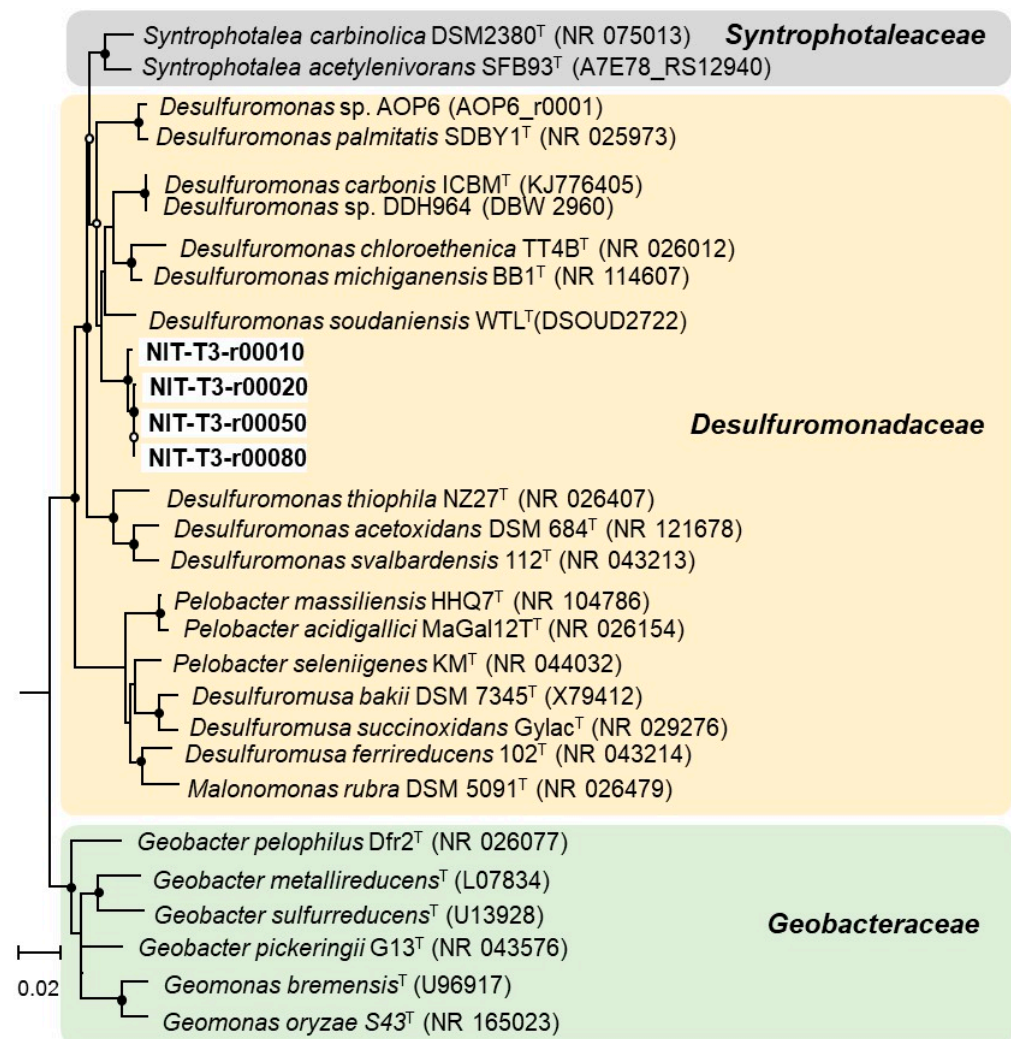


Figure 2. Phylogenetic tree generated using 16S rRNA gene sequences of members of Desulfuromonadales. Closed and open circles indicate bootstrap > 80% and 60%, respectively. GenBank accession numbers are stated in parentheses.

Strain NIT-T3 grew at 10–35 °C (optimum, 25 °C), pH 6.4–8.4 (optimum pH 6.8–7.1), and tolerated 0.05–3% NaCl (optimum, 0.2–1%) (Table 1). Growth was completely inhibited at concentrations of $\geq 3\%$ NaCl. Strain NIT-T3 could metabolize hydrogen, formate, acetate, lactate, pyruvate, succinate, malate, peptone, isopropanol, and yeast extract in the presence of nitrate (Table 1). Lactate, pyruvate, succinate, and the combination of H₂ and acetate resulted in optimal growth together with nitrate. No growth occurred in the presence of butyrate, glucose, glycerol, ethanol, isobutyrate, caproate, benzoate, phenol, methanol, butanol, or fructose. Cells did not show any apparent movement on a slide, suggesting that the strain NIT-T3 was non-motile.

Table 1. Cont.

Characteristic	1	2	3	4	5	6	7	8	9	10
Major fatty acids (>10%)	C _{16:1} ω _{7c} (26.2%) C _{16:0} (18.3%) C _{15:0} (13.2)	ND	C _{16:0} (39.3%) C _{16:1} ω _{7c} and/or iso-C _{15:0} 2-OH (36.6%)	C _{16:0} (43%) C _{16:1} ω _{7c} (35%) C _{15:0} (10%)	ND	ND	ND	ND	ND	ND
Major respiratory quinones	MK-8 (93%) MK-9 (5.3%) MK-7 (1.9%)	ND	ND	ND	ND	ND	ND	ND	ND	ND

Strains: 1, NIT-T3 (this study); 2, *Desulfuromonas soudanensis* WTL^T [21]; 3, *Desulfuromonas carbonis* ICBM^T [18]; 4, *Desulfuromonas svalbardensis* 112^T [17]; 5, *Desulfuromonas michiganensis* BB1^T [16]; 6, *Desulfuromonas chloroethenica* TT4B^T [15]; 7, *Desulfuromonas thiophila* NZ27^T [14]; 8, *Desulfuromonas palmitatis* SDBY1^T [13]; 9, *Desulfuromonas acetexigens* 2873^T [12]; 10, *Desulfuromonas acetoxidans* DSM 684^T [11]. The data for NIT-T3 was obtained in this study and others are brought from references [14–21].

+, good growth; (+), hydrogen was oxidized but no growth; -, no growth; [motile], only a small population was motile; ND, not determined; NM, not motile; temp., temperature; AQDS, Anthraquinone-2,6-disulfonate; GO, graphene oxide.

* Tested with acetate and fumarate as the substrates.

3.3. Physiological and Biochemical Characterization

Similar to most *Desulfuromonas* species, strain NIT-T3 showed respiration using sulfur and ferric iron coupled with acetate oxidation. Contrary to the lack of nitrate respiration in other *Desulfuromonas* members, strain NIT-T3 exhibited nitrate respiration (Figure 3). The cell density increased from 5.7×10^7 to 2.4×10^8 cells/mL with a reduction of 5.1 mM of nitrate within 7 d of incubation. Meanwhile, a maximum concentration of 1.7 mM of nitrite was produced in the medium. The NIT-T3 did not grow in the culture supplemented with nitrite. These results indicated the ability of strain NIT-T3 to grow on nitrate, while reducing nitrate to nitrite. The imbalance of the spiked nitrate and produced nitrite suggested the assimilative utilization of nitrite as nitrogen source.

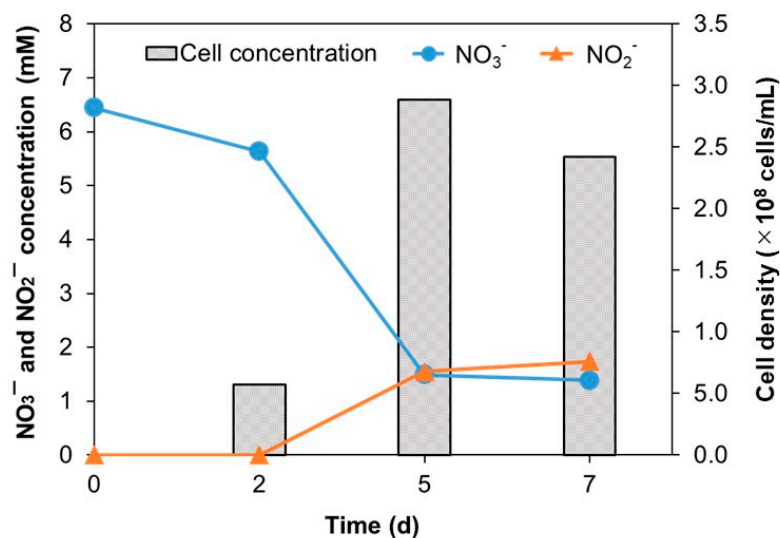


Figure 3. Changes in the NO₃⁻ and NO₂⁻ concentrations and NIT-T3 cell densities in the culture supplemented with nitrate.

3.4. Chemotaxonomic Characterization

The major fatty acids identified in strain NIT-T3 were C_{16:1}ω7c (26%), C_{16:0} (18%), and C_{15:0} (13%) (Table 1). The fatty acid profile of *Desulfuromonas* species is available for only two strains, *D. svalbardensis* 112^T [20] and *D. carbonis* ICBM^T [21]; these two strains contain the three major fatty acids found in strain NIT-T3. However, the proportions differ among the three strains. The most abundant fatty acid is C_{16:0} (approximately 40%) in strains 112^T and ICBM^T, and C_{15:0} in ICBM^T is detected in minor amounts (0.1%). The presence of C_{16:1}ω7c and C_{16:0} as main cellular fatty acids was common in most members of *Geobacter* [43–47] rather than in only *Desulfuromonas*.

The major respiratory quinones in NIT-T3 were identified as MK-8 (93%), and other menaquinones including MK-7 (1.9%) and MK-9 (5.3%) were detected. This result is consistent with the fact that MK-8 is a typical respiratory quinone present in the genus *Geobacter* [43,44,47,48], although the menaquinone profile data of other species of the genus *Desulfuromonas* are not available.

3.5. General Genomic Features

NIT-T3 contained a single 4,656,376 bp circular chromosome that encodes 4119 protein-coding sequences (CDS), 60 transfer RNAs, 1 transfer-messenger RNA, and 10 rRNAs. The G + C content in strain NIT-T3 was approximately 63.1%, which is similar to that of *D. acetexigens* 2873^T and *D. acetoxidans* (Table 1). The genome map is shown in Figure 4. Regarding energy conversion, NIT-T3 had CDSs to metabolize hydrogen, lactate, pyruvate, and other organic acids of the TCA cycle intermediates (fumarate, succinate, malate), and complete TCA cycle. NIT-T3 also contained a full set of genes associated with glycolysis similar to the other two strains; however, the bacteria cannot utilize glucose due to the lack

of glucose transporters [25]. A gene encoding nitrate reductase (*NarB*) was found which oxidizes quinol and reduces nitrate to nitrite. The reductive acetyl-CoA pathway and reductive TCA cycle lacked certain genes, suggesting an inability of the strain to fix carbon.

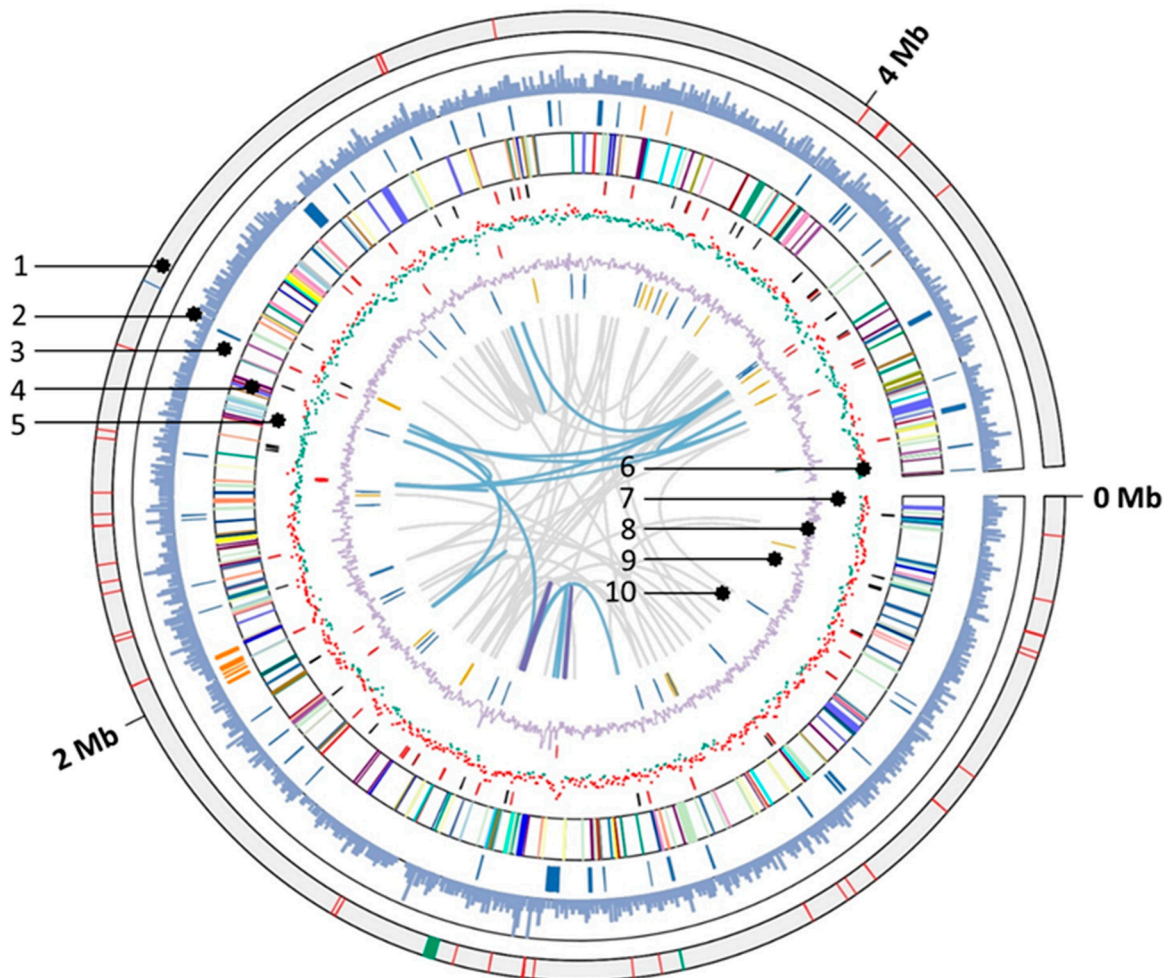


Figure 4. Features of the complete genome of '*Desulfuromonas versatilis*' NIT-T3. Circular representation of the genome was generated using TBtools v.1.082 [49]. Rings numbered from the outside to inside are: 1, location of tRNA (red), transfer messenger RNA (blue), and rRNA (green); 2, gene density; 3, *c*-type cytochromes (blue), and type IV pili (orange); 4, protein coding sequences colored based on KEGG category; 5, putative sensor histidine kinases (red) and response regulators (black); 6, G + C skew (red, positive; green, negative) approximated using GenSkew (<http://genskew.csb.univie.ac.at/>); 7, transposase (red) and phage integrase (black); 8, G + C content; 9, genes unique to NIT-T3 (orange, annotated; blue, unannotated) compared to other *Desulfuromonas* spp; 10, links showing repetitive sequence $\geq 95\%$ identity (cyan, > 500 bp; purple, > 2 kbp). KEGG, Kyoto Encyclopedia of Genes and Genomes.

3.6. Putative *c*-Type Cytochromes

NIT-T3 possessed 79 putative *c*-type cytochromes. The CDSs with $C(X)_nCH$, $n = 2-4$, were first screened and then identified as *c*-type cytochromes either based on the presence of a conserved domain of *c*-type cytochromes in the pfam and TIGR databases (e-value = < 0.01 cutoff) or showing an e-value $< 10^{-10}$ in the pairwise alignment with *c*-type cytochromes of strain PCA. Among them, 61 were homologs of *c*-type cytochromes in *Desulfuromonas* strains (Figure 5, $\geq 40\%$ amino acid identity (AAI) in the 759–92 AAs of the HIPER scoring region) and 38 were homologs of those in *Geobacter sulfurreducens* PCA, a well-characterized model of iron-reducing bacterium. NIT-T3 contained a relatively larger number of *c*-type cytochromes than other *Desulfuromonas* strains in the range from 37 to 44. Based on PROSITE prediction [50], most of the *c*-type cytochromes were present

in the periplasmic (28), extracellular (7), and cytoplasmic membranes (6), whereas a few cytochromes were present in the cytoplasm (3). The number of heme-binding motifs varied, and ranged from 1 to 53.

Tag	Number of		Local-ization	Closest protein in strains				Closest protein in database			
	CX _n CH	n=3		PCA1	DDH964	AOP6	WTL	Accession		Phylogeny of origin	
								n=2	20-30	30-40	41-60
3570	5	0	CM	OmcV, 1996	-	-	2438	FD174_3512	Geo	-	-
3730	4	0	-	PpcD, 1024	2382	1767	2694	C0619_13365	Des	Desl	-
4810	2	0	CM	CcoP, 2513	2374	0638	2315	C0615_07200	Des	Desl	-
5430	53	0	PP	OmcX, 0670	301	1132	2958	WP_040198997	Geo	Geoa	subterraneus
5440	12	0	PP	ExtA, 2645	-	1132	-	ENN94_00220	Geo	Geoa	subterraneus
5490	10	0	-	ExtG, 2724	1658	-	823	IH614_00830	-	-	-
6100	18	0	PP	CytT, 2299	833	982	2629	C0623_04030	Des	Desl	-
7890	1	0	PP	-	839	2693	601	DSOUD_0601	Des	Desl	soudanensis
7900	3	0	CP	-	-	-	-	BA871_12945	-	-	-
8600	8	0	EX	OmcZ, 2076	-	-	-	GFER_11920	Geo	Geoa	ferrihydriticus
8630	2	0	-	Dhc2, 2927	3061	2447	649	C0614_03360	Des	Desl	-
9000	3	0	PP	PpcD, 1024	1072	1210	3086	IBX47_10010	-	-	-
9780	6	0	PP	2211	2875	115	2475	DBW_2875	Des	Desl	-
9980	12	0	PP	615	2851	1175	2958	FL622_12825	Des	Desl	acetexigens
10000	8	0	PP	CtcB, 0616	2849	1668	2956	A2X84_08365	Des	-	-
10020	4	0	EX	OmcE, 0618	2847	1181	2954	C0621_05920	Des	Desl	-
10580	7	1	-	3218	2851	1175	2958	C0622_11315	Des	Desl	-
10590	12	0	-	670	-	1173	-	HPP94_15845	-	-	-
10600	10	2	EX	3226	3049	1181	663	C0619_06915	Des	Desl	-
10630	5	0	-	ExtT, 3223	2851	1178	2958	GSVR_15810	Geo	Geob	-
10650	13	1	PP	3218	2851	1175	2958	ENR76_08625	Geo	-	-
10660	10	0	EX	OmcB, 2737	2625	2385	-	GM21_3565	Geo	Geob	-
10670	18	0	PP	OmcB, 2737	3049	2432	2970	GPELO_01f5367	Geo	Geob	pelophilus
10680	4	0	PP	CtcA, 3221	2847	1176	2954	GSVR_15740	Geo	Geob	-
10700	22	0	EX	OmcB, 2737	2625	2432	-	C0619_07865	Des	Desl	-
10710	4	0	PP	CtcA, 3221	2847	1176	2954	GSVR_15740	Geo	Geob	-
12140	5	0	-	CbcX, 1648	2721	764	2440	C0617_08690	Des	Desl	-
15020	2	0	-	-	-	-	-	-	-	-	-
15500	2	0	PP	1538	-	104	3080	DCZ63_04680	Geo	Geob	-
15840	8	0	PP	-	1324	-	1989	GQ530_06150	-	-	-
16340	1	0	-	-	3541	-	3220	SAMN05660420_00810	Des	Desl	kysingii
18560	3	0	PP	PpcD, 1024	1072	1210	3086	JXR59_05200	Des	-	-
19090	1	0	-	CycC, 1740	1735	-	-	C0623_12135	Des	Desl	-
20270	7	0	PP	3214	-	-	-	B5V00_09970	Geo	Geot	hydrogeniphilus
20370	9	1	PP	OmcI, 1228	1987	1517	3216	AOP6_1517	Des	Desl	-
21530	7	0	PP	-	-	87	1849	DSOUD_1849	Des	Desl	soudanensis
23710	4	0	-	3154	-	1033	150	DSOUD_0150	Des	Desl	soudanensis
23720	4	0	-	NrfH, 3155	-	1033	151	GeB_11375	Geo	Geoa	subterraneus
26390	4	0	EX	OmcP, 2913	3049	1181	663	-	Geo	Geop	electrodiphilus
26400	35	2	-	2884	3048	-	664	-	Geo	Geoa	subterraneus
26410	15	1	-	OmcN, 2898	3039	-	665	FO488_05880	Geo	Geob	-
26420	21	1	EX	OmcN, 2898	3047	-	665	DBW_3047	Des	Desl	-
26940	12	0	PP	OmcM, 2935	-	659	-	C0617_13980	Des	Desl	-
27260	1	0	-	-	-	-	2537	-	-	-	-
27920	4	0	PP	PpcD, 1024	2382	1063	2694	DSOUD_2694	Des	Desl	soudanensis
28400	7	1	CP	1786	2445	1182	2414	A2X84_02795	-	-	-
28410	4	0	-	1787	2446	1181	2415	-	Geo	Geop	electrodiphilus
29000	2	0	-	-	-	-	-	GW001_04425	-	-	-
29420	6	0	PP	CytT, 2299	833	2967	2629	ENQ87_05415	Geo	Geob	metallireducens
29940	12	0	PP	ExtA, 2645	-	1133	-	C0616_11920	Des	Desl	-
29950	12	0	PP	OmcX, 0670	-	1132	-	WP_140396673	Des	-	-
30630	13	0	-	OmcB, 2737	3210	456	-	-	Des	Desl	-
30640	10	0	PP	OmaB, 2738	3211	457	-	-	Des	Desl	-
30830	4	0	-	-	-	-	-	-	-	-	-
31280	2	0	CM	CoxB, 0222	3011	0614	RS04825	WP_148895441	Geo	Geot	ehrichii
31490	4	0	-	CbcR, 2930	-	654	-	IH614_13215	-	-	-
31530	10	0	-	CbcM, 2934	-	658	-	C0617_16150	Des	Desl	-
31540	12	0	-	CbcM, 2935	3210	659	2970	C0618_06315	Des	Desl	-
31560	5	0	-	ExtK, 2937	-	662	-	IH613_02405	-	-	-
31880	1	0	CM	Cyc1, 3334	948	615	963	C0617_01390	Des	Desl	-
35490	5	0	CP	CtcC, 2801	-	276	-	HGB35_03625	Geo	-	-
36250	9	0	-	ExtD, 2642	2791	-	704	ENR76_02965	Geo	-	-
36260	5	0	-	ExtCF, 2643	2792	-	2914	ED859_04185	-	-	-
36350	1	0	-	1397	2137	-	-	IH614_16780	-	-	-
36530	1	0	-	PpcC, 0365	2382	1768	2694	IH614_03740	-	-	-
37260	7	0	-	CbcA, 0594	-	2567	1253	-	Des	Desl	acetexigens
37510	3	0	-	OmcV, 1996	2875	2520	2475	FL622_16595	Des	Desl	acetexigens
38420	10	0	PP	OmaB, 2738	3211	457	-	DBW_2626	Des	Desl	-
38430	12	0	EX	OmcB, 2737	2625	2432	-	C0614_09110	Des	Desl	-
38440	10	0	PP	OmaB, 2738	3211	456	-	DBW_2626	Des	Desl	-
38450	10	0	-	OmcB, 2737	0.3379	2432	-	GSU2737	Geo	Geob	sulfurreducens
38460	10	0	-	-	3209	-	887	C0617_16065	Des	Desl	-
39480	1	0	-	-	3572	2837	81	FIB02_09325	Des	Desl	-
40040	9	0	CM	CbcL, 0274	421	128	214	A2X84_12435	Des	-	-
40060	4	0	-	CbcS, 0068	415	-	211	A2X84_05300	Des	-	-
40090	5	1	CM	ImcH, 3259	412	110	207	DBW_0412	Des	Desl	-
40120	2	0	PP	MaaA, 0466	1968	558	RS12400	WP_092058305	Des	Desl	acetexigens
40720	4	0	PP	NrfA, 3154	-	1033	150	TRO77878	Des	Desl	acetoxidans
41160	2	0	-	3332	13	12	3572	PLX84049	Des	Desl	-

Figure 5. List of putative *c*-type cytochrome C proteins present in the NIT-T3 genome. Tag indicates the locus tag of the coding sequence encoding *c*-type cytochromes in the genome. CM, cytoplasmic membrane; PP, periplasm; EX, extracellular; (-), unknown. The number and color scale for the closest protein in the strain indicates the locus tag and amino acid identity (%), respectively. Geo, *Geobacteraceae*; Geoa, *Geoalkalibacter*; Geob, *Geobacter*; Geop, *Geopsychrobacter*; Geot, *Geothermobacter*; Syn, *Syntrophotaleaceae*; Synt, *Syntrophotalea*; Des, *Desulfuromonadaceae*; Desl, *Desulfuromonas*.

The *c*-type cytochromes were highly variable showing approximately ~77.76% similarity to those of *Desulfuromonas* strains. The phylogeny matched within families of *Geobacteraceae* and *Desulfuromonadaceae*, and few were related to cytochromes found only

in metagenomes. Among them, six *c*-type cytochromes were unique and shared <40% AAI with those in the database; four independent genes (DESUT3_0860, 20270, 29420, DESUT3_29000), and two (DESUT3_10660, 38460) were present in gene clusters of putative cytochromes (Figure 6).

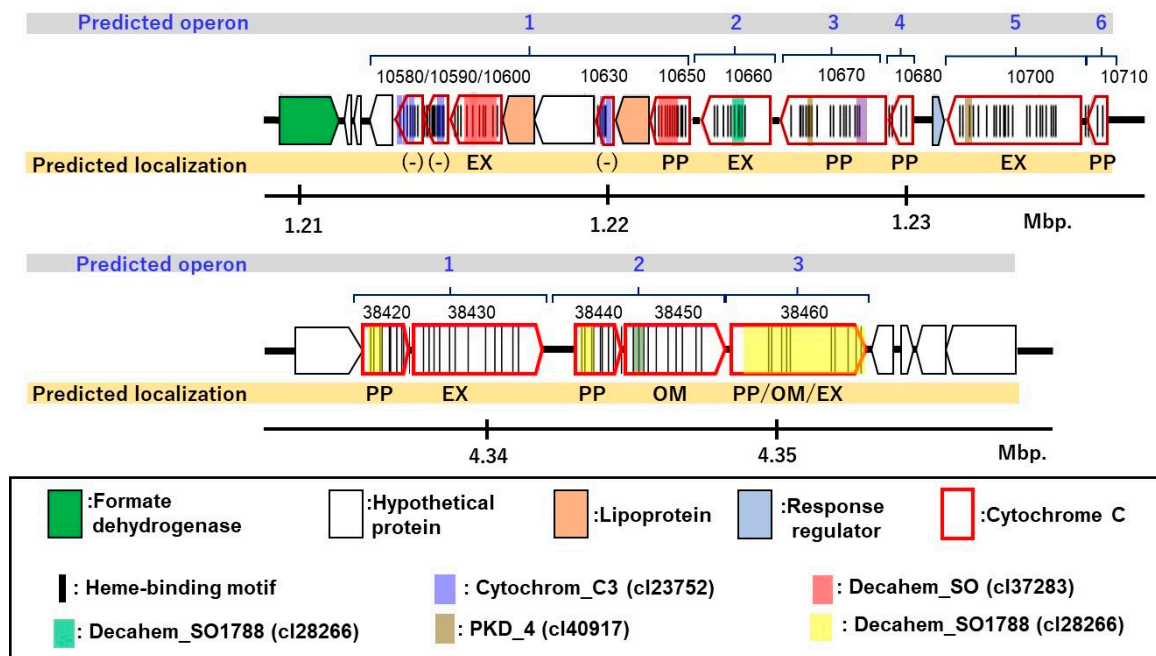


Figure 6. Two predicted gene clusters of unique *c*-type cytochrome C in strain NIT-T3.

3.7. Homologs of *c*-Type Cytochromes to Those in *G. sulfurreducens* PCA

Twenty-four *c*-type cytochromes were homologs of those functionally identified in *G. sulfurreducens* PCA. DESUT3_09000, 18560, and 27920 are homologous to PpcD, DESUT3_10670 and 38450 are homologous to OmcB, and DESUT3_40090 and 40040 are homologous to ImcH and CbcL present in *G. sulfurreducens*, respectively. These cytochromes are involved in the porin-cytochrome (Pcc) EET pathways that mediate electron transfer across the cell envelope [51]. In the Pcc pathways, ImcH and CbcL represent inner membrane cytochromes that oxidize quinol in the cytoplasmic membrane and transfer the released electrons to the periplasmic PpcA/PpcD [52,53]; PpcA/PpcD transfers the electrons acquired from the cytoplasm to the OmcB-based (ombB-omaB-omcB) conduit in the outer membrane [54]. The OmcB-based conduit transfers electrons through the lipid bilayer of proteoliposomes and directly reduces Fe(III) hydroxides outside the proteoliposomes [55,56].

DESUT3_29940, 36260, 05490, 10630, and 31560 are homologs of ExtA, ExtC, ExtG, ExtT, and ExtK of *G. sulfurreducens*, respectively. They belong to the outer membrane electron conduit *ext* gene clusters, which transfer electrons across the outer membrane to the bacterial surface [57]. DESUT3_31530 and 31540 are homologs of CbcM, and DESUT3_37260, 31490, 40060, and 12140 are homologs of CbcA, CbcR, CbcS, and CbcX of *G. sulfurreducens*, respectively. These Cbc-proteins and CbcL constitute the menaquinol oxidoreductase protein complexes, which combine electron transfer processes to form a proton gradient across the inner membrane via either a Q loop or a Q cycle [58,59].

DESUT3_40120 is a homolog of the inner-membrane-associated diheme cytochrome MacA of *G. sulfurreducens*, which is described as a peroxidase that can also mediate the electron transfer between inner membrane components and multiheme periplasmic cytochromes [60]. DESUT3_20370, 37510, and 29950 are homologs of the outer membrane cytochrome OmcI, OmcV, and OmcX of *G. sulfurreducens*, respectively. These Omc-proteins help transfer the electrons extracellularly, are required for Fe (III) reduction [61,62], and

are significantly upregulated by Fe(III) oxides/Mn(IV) oxides/granular activated carbon [61,63]. DESUT3_40720 is a homolog of NrfA, which functions as a nitrite reductase component in a putative NrfH/NrfA nitrite-to-ammonia respiration pathway [25]. DESUT3_31280 is a homolog of CoxB encoding a cytochrome c oxidase subunit II, which is involved in the oxidative phosphorylation pathway.

3.8. Type IV Pilus (T4P)-Related Genes

The strain NIT-T3 was found to contain 16 CDSs encoding T4P (Figure 7) and 3 related genes including transcription regulators. T4P are filamentous polymers of pilin monomers that undergo dynamic rapid polymerization and depolymerization from a pool of pilin [64]. The pilus polymer of pilin protein PilA of *G. sulfurreducens* PCA is an electrically conductive pilus and is known to be involved in the EET of solid electron acceptors [65]. Aromatic acids are key elements associated with conductivity and are estimated to account for 9.83% of the content in the PilA of strain PCA [66]. The aromatic acid content in the PilA homolog in NIT-T3 was 14.2%, which was relatively high based on the range of PilA aromatic acid content in phylogenetically diverse bacteria (5.5–25.25%) [67]; this suggested that the polymer may be conductive. The NIT-T3 genome was found to contain a full set of genes encoding T4P: two major pilins PilA and PilE, four minor pilins PilE, PilY, PilV, and PilW, and other essential proteins for the secretin (PilQ), alignment (PilM, PilN, PilO, and PilP), platform (PilC), four retraction ATPases (PilT), and assembly ATPases (PilB). Most CDSs are well-conserved in the genus *Desulfuromonas*, except for CDSs of four minor pilins closely related to the genera *Syntrophotalea* (PilE, PilV, and PilW) and *Geobacter* (PilY).

Tag	Anotation	aromatic acid Mole%	Closest protein in strains				Closest protein Protein tag	16SrRNA-gene phylogeny		
			PCA1	DDH964	AOP6	WTL		Family	Gen.	Species
17090	type IV pilin PilY	11.7	GSU1066	DBW_1432	AOP06_2015	DSOUD2166	GPICK_05505	Geo	Geob	pickeringii
17180	type IV pilin PilV	5.81	-	-	-	-	Pcar_2158	Syn	Synt	carbinolica
17190	type IV pilin PilW	8.12	-	DBW_3171	AOP06_2014	-	Pcar_2157	Syn	Synt	carbinolica
17220	type IV pilin PilE	8.66	-	-	AOP06_0499	DSOUD2405	Pcar_2154	Syn	Synt	carbinolica
17280	type IV pilus assembly ATPase PilB		GSU1491	DBW_1442	AOP06_2007	DSOUD2162	DSOUD2162	Des	Desl	soudanensis
17290	type IV twitching motility protein PilT		GSU1492	DBW_1443	AOP06_2006	DSOUD2161	DBW_1443	Des	Desl	-
17300	type IV pilus assembly protein PilC		GSU1499	DBW_1443	AOP06_2005	DSOUD2160	DBW_1443	Des	Desl	-
17330	type IV pilin PilA	14.2	GSU1496	DBW_1447	AOP06_2002	DSOUD2157	WP_092053366.1	Des	Desl	acetexigens
17480	type IV pilus assembly protein PilM		GSU2032	DBW_1445	AOP06_1988	DSOUD2151	WP_092053366.1	Des	Desl	acetexigens
17490	type IV pilus assembly protein PilN		GSU2031	DBW_1446	AOP06_1987	DSOUD2150	DBW_1446	Des	Desl	-
17500	type IV pilus assembly protein PilO		GSU2030	DBW_1457	AOP06_1986	DSOUD2149	WP_092053361.1	Des	Desl	acetexigens
17510	type IV pilus assembly protein PilP		GSU2029	DBW_1458	AOP06_1985	DSOUD2148	DSOUD2148	Des	Desl	-
17520	type IV pilus modification protein PilQ		GSU2029	DBW_1458	AOP06_1985	DSOUD2148	AOP06_1985	Des	Desl	-
32370	type IV twitching motility protein PilT		GSU0146	DBW_0920	AOP06_0579	DSOUD0931	WP_092054494.1	Des	Desl	acetexigens
32890	type IV twitching motility protein PilT		GSU0230	DBW_0856	AOP06_0536	DSOUD0328	WP_072909266.1	Des	Mal	rubra
37530	type IV twitching motility protein PilT		GSU0146	DBW_0920	AOP06_0579	DSOUD0931	WP_092055312.1	Des	Desl	acetexigens

Figure 7. List of T4P assembly-related genes in the NIT-T3 genome. Tag indicates the locus tag of coding sequences encoding T4P-related proteins in the genome. The number and color scale for the closest protein in the strain indicates the locus tag and amino acid identity (%), respectively. T4P, Type IV pilli; Geo, Geobacteraceae; Geob, *Geobacter*; Syn, *Syntrophotaleaceae*; Synt, *Syntrophotalea*; Des, *Desulfuromonadaceae*; Desl, *Desulfuromonas*; Mal, *Malonomonas*.

4. Discussion

The isolation of a novel electrogenic strain NIT-T3 of the genus *Desulfuromonas* and its respiration-ability specific to solid minerals suggests the adaptation of the genus to solid minerals or conductor-driven metabolism [8–13]. The ability to grow on solid minerals and electrodes is supported by the presence of seven extracellular *c*-type cytochromes (Figure 5), and conductive pilin (PilA)-homologs and full sets of T4P-assembly genes in the genome (Figure 6). These CDSs are phylogenetically cross-related in the order *Desulfuromonadales* beyond family, and show higher identities with CDSs of the genera *Desulfuromonas* and *Malonomonas* of the family *Desulfuromonadaceae*; *Geobacter*, *Geokalibacter*, and *Geopsychrobacter*

of the family *Geobacteraceae*, and *Syntrophotalea* of family *Syntrophotaleaceae*. The fact that all members in these genera are capable of reducing solid minerals, and that the EET-related genes are closely related suggests the early divergence of EET during the evolution of bacteria in the order *Desulfuromonadales*. The strain NIT-T3 required NaCl and showed growth in the presence of 0.05–3.0% NaCl; the preference for NaCl was in agreement with the salt tolerance observed in the genus *Desulfuromonas* (0–3.0%) [17,19,21]. This supports the fact that *Desulfuromonas* species have widely adapted to both marine and freshwater environments.

The *c*-type cytochromes were hypervariable and abundant ($n = 79$), whereas other *Desulfuromonas* strains are reported to contain 37–44 *c*-type cytochromes according to the given annotation. The difference in the number was probably due to the difference in annotation strategies. A CDS for *c*-type cytochrome (DESUT3_5430) had 53 heme-binding sites which was the maximum number, and showed 54% of the closest identity to that of *Geoalkalibacter subterraneus* (B_0221) and 49% and 41% with that of contigs of *D. acetexigens* and *M. rubra*, respectively. The number of heme-binding sites in these homologs ranged from 55 to 77, indicating the broad distribution of the *c*-type cytochrome with such a large number of heme-binding sites in the order *Desulfuromonadales*.

Among the unique *c*-type cytochromes, two cytochromes (DESUT3_10660 and DESUT3_38460) were present in gene clusters including multiple *c*-type cytochromes (Figure 7). The gene cluster harboring DESUT3_10660 contains ten non-cytoplasmic *c*-type cytochromes with domains for cytochrome_C3 (cl23752), decahem_SO (cl37283), and decahem_SO1788 (cl28266). Three homologs of *c*-type cytochromes are found in strain PCA: DESUT3_10630 sharing 49% identity with ExtT which is a subunit of ExtTUVW conduit, and DESUT3_10680 and DESUT3_10710 with both sharing 43% identity with CtcA and tetra/tri-heme *c*-type cytochromes, respectively. DESUT3_38460 was located in a gene cluster including five CDSs of *c*-type cytochromes: three CDSs (DESUT3_38420, 38440, and 38450) shared 41–69% similarity with the *c*-type cytochrome of *Desulfuromonas* strains, and DESUT3_38430 showed 53% similarity with a hypothetical protein of *Desulfuromusa kysingii*. Among them, only one CDS (DESUT3_38450) was the homolog of the functionally identified *c*-type cytochrome known as omcB, a subunit of the OmaB/OmbB/OmcB conduit. The function of these gene clusters is unknown; however, it is speculated that they are essential for the unique adaptation of the strain for facilitating EET.

Strain NIT-T3 could metabolize nitrate which is not observed in other strains in the genus *Desulfuromonas*. The strain NIT-T3 produced nitrite; however, its production was approximately one-third of the amount of nitrate supplemented (Figure 3). The difference in the concentrations of produced nitrite and supplemented nitrate may be attributed to the assimilation of ammonia produced from nitrite. Analysis of the genome of NIT-T3 indicated the possibility of nitrite-to-ammonia transformation. Similar to NIT-T3, the complete genomes of all four *Desulfuromonas* strains contain CDSs for the nitrogen fixation pathway, including nitrite-to-ammonia reduction. However, genes encoding transporters for the uptake of extracellular nitrate were present in NIT-T3 alone (Figure 8A). This is consistent with the fact that NIT-T3 alone, and not the other *Desulfuromonas* strains, could reduce nitrate.

The NIT-T3 genome was found to contain several unique CDSs that encode complete metabolic pathways which are absent in the other three *Desulfuromonas* genomes: histidine degradation to glutamate (Figure 8B), and C1-unit interconversion (Figure 8C). This suggested a variable metabolism in members of the genus *Desulfuromonas* associated with the transient reduction and uptake of genes in the genome.

In addition to the unique genes mentioned above, NIT-T3 possesses 46 other CDSs in the genome with no confirmed homologs (<40%) in other species of the *Desulfuromonas* strains; 29 of these sequences encode proteins with predicted functional annotation (Table S1). The unique proteins include a putative autoinducer-2 (AI-2) transporter family protein (DESUT3_07100), which has been reported to regulate the intracellular concentration of AI-2, a quorum-sensing chemical that affects global gene expression in biofilms [68,69] and

shares a higher identity with proteins of *Geobacter* species than those of *Desulfuromonas*. The NIT-T3 genome includes another candidate for the AI-2 transporter family protein (DESUT3_31000) that was similar to that in all three genomes of the genus *Desulfuromonas*, but not to that of *Geobacter* species (63–70% identity). These two paralogs of AI-2 transporters with different phylogenies may potentially control biofilm growth. DESUT3_07210 encodes RNA molecules of a labile antitoxin, HicB, that regulates the expression of a toxin protein, HicA. Both proteins are involved in bacterial survival under stress conditions, such as nutrient deprivation and antibiotics [68,69]. An additional set of CDSs for HicAB was present in the genome; however, its role in *Desulfuromonadales* has never been investigated. Several metabolic genes (DESUT3_29720, 35500, 33690, and 37760) were also found to be unique to the NIT-T3 genome; however, these genes are disconnected from other functional genes and do not complete a series of metabolic processes.

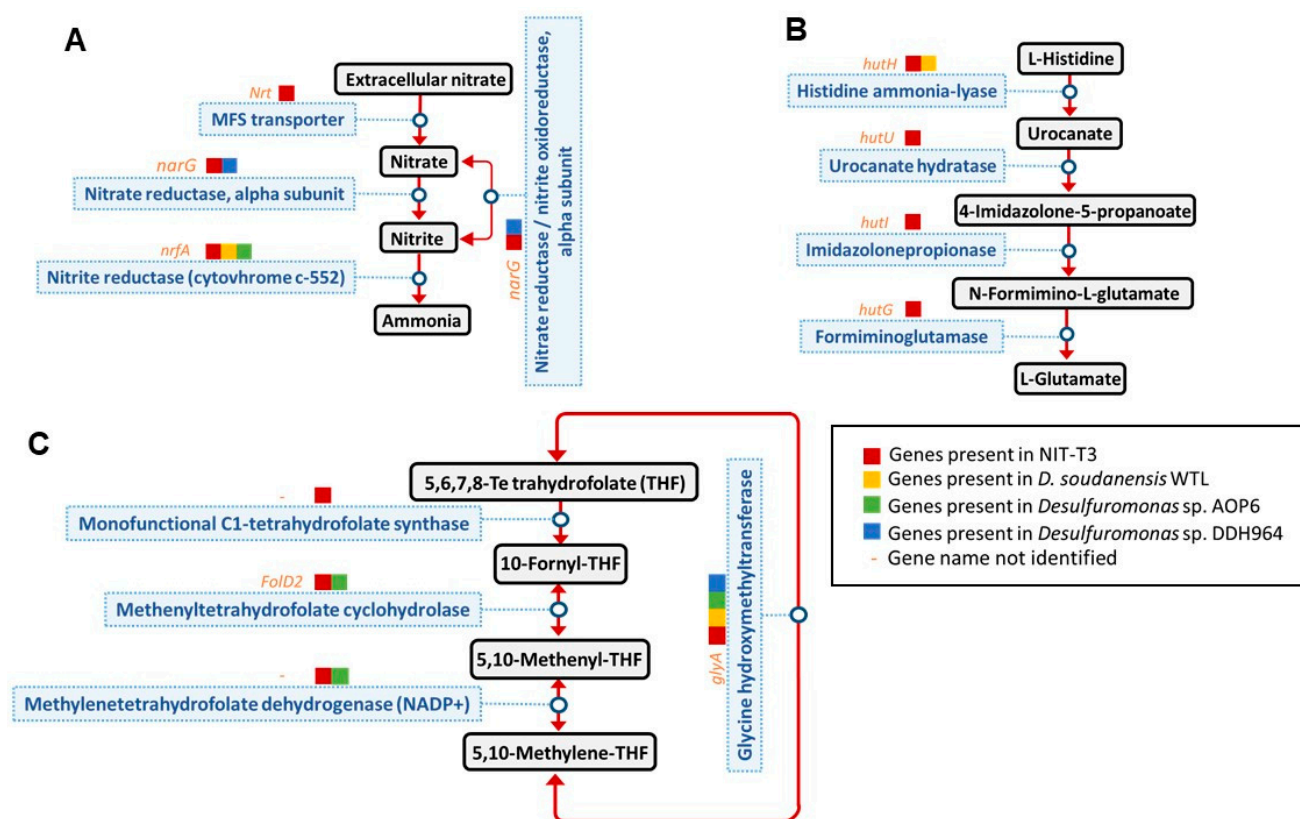


Figure 8. The complete metabolic pathway of strain NIT-T3 distinct from that of the complete genomes of three *Desulfuromonas* strains. Metabolic pathways of (A) nitrate reduction, (B) histidine degradation, and (C) C1-unit interconversion.

5. Conclusions

The isolation and polyphasic characterization of the novel strain NIT-T3 revealed an increase in the metabolic capability of the genus *Desulfuromonas*. In total, 79 of the large number of *c*-type cytochromes suggested their substantial role as representative electrogenic bacteria in natural and synthetic environments. The interswitching phylogeny of EET-related genes in members of the order *Desulfuromonadales* beyond the family suggested the early divergence and the substantial roles of the order *Desulfuromonadales* rather than the specific genus like *Geobacter* in EETs in various environments. Strain NIT-T3 is proposed as a new species of the genus *Desulfuromonas* according to the phenotype and phylotype and the description is provided as follows:

Description of *Desulfuromonas versatilis* sp. Nov.

Desulfuromonas versatilis (ver.sa'ti.lis L. masc./fem. Adj. versatilis, versatile with respect to the capability to use a variety of electron donors and acceptors).

Cells are Gram-negative, non-spore-forming, rod-shaped, non-motile, and strictly anaerobic. Optimal growth was observed at 25 °C, pH 6.8–7.1, and NaCl concentration ranging from 0.2% to 1%. The substrates used for nitrate reduction included hydrogen, formate, acetate, lactate, pyruvate, succinate, malate, isopropanol, peptone, and yeast extract. Elemental sulfur, iron oxide, fumarate, nitrate, AQDS, malate, graphite electrode, and GO served as terminal electron acceptors coupled to acetate oxidation. The major cellular fatty acids present were C_{16:1}ω7c and C_{16:0}, and the major respiratory quinone in the cell wall of NIT-T3 was MK-8. The type strain, NIT-T3^T was isolated from a mixture of seawater and coastal sand. The genomic G + C content in the type strain was 63.1%.

Supplementary Materials: The following are available online at <https://www.mdpi.com/article/10.3390/microorganisms9091953/s1>, Table S1: Genes uniquely present in strain T3 compared with other species of the genus *Desulfuromonas*.

Author Contributions: L.X.: Data analysis and writing; N.Y.: isolation, data curation, conceptualization, writing, supervision, funding acquisition; S.I., data analysis; L.M., data curation and data analysis. All authors have read and agreed to the published version of the manuscript.

Funding: This study received funding from MEXT/JSPS KAKENHI (grant numbers: 18K18876 and 16H06279) and the JSPS Joint Research Program with NSFC. The genome analysis was supported by MEXT KAKENHI (No. 221S0002).

Institutional Review Board Statement: Not applicable.

Informed Consent Statement: Not applicable.

Data Availability Statement: The data presented in this study are available on request from the corresponding author.

Acknowledgments: We would like to thank Tomomi Suzuki and Asuka Akita for their technical support in the cultivation and genomic experiments.

Conflicts of Interest: The authors declare no conflict of interest.

References

1. Logan, B.E.; Hamelers, B.; Rozendal, R.; Schröder, U.; Keller, J.; Freguia, S.; Aelterman, P.; Verstraete, W.; Rabaey, K. Microbial fuel cells: Methodology and technology. *Environ. Sci. Technol.* **2006**, *40*, 5181–5192. [[CrossRef](#)]
2. Zou, S.; He, Z. Efficiently “pumping out” value-added resources from wastewater by bioelectrochemical systems: A review from energy perspectives. *Water Res.* **2018**, *131*, 62–73. [[CrossRef](#)] [[PubMed](#)]
3. Wang, X.; Aulenta, F.; Puig, S.; Esteve-Núñez, A.; He, Y.; Mu, Y.; Rabaey, K. Microbial electrochemistry for bioremediation. *Environ. Sci. Ecotechnol.* **2020**, *1*, 100013. [[CrossRef](#)]
4. Zhi, W.; Ge, Z.; He, Z.; Zhang, H. Methods for understanding microbial community structures and functions in microbial fuel cells: A review. *Bioresour. Technol.* **2014**, *171*, 461–468. [[CrossRef](#)] [[PubMed](#)]
5. Saheb-Alam, S.; Persson, F.; Wilén, B.M.; Hermansson, M.; Modin, O. Response to starvation and microbial community composition in microbial fuel cells enriched on different electron donors. *Microb. Biotechnol.* **2019**, *12*, 962–975. [[CrossRef](#)] [[PubMed](#)]
6. Wu, H.; Yang, M.; Tsui, T.-H.; Yin, Z.; Yin, C. Comparative evaluation on the utilization of applied electrical potential in a conductive granule packed biotrickling filter for continuous abatement of xylene: Performance, limitation, and microbial community. *J. Environ. Manag.* **2020**, *274*, 111145. [[CrossRef](#)] [[PubMed](#)]
7. Katuri, K.P.; Kamireddy, S.; Kavanagh, P.; Mohammad, A.; Conghaile, P.; Kumar, A.; Saikaly, P.E.; Leech, D. Electroactive biofilms on surface functionalized anodes: The anode respiring behavior of a novel electroactive bacterium, *Desulfuromonas acetexigens*. *bioRxiv* **2020**. [[CrossRef](#)]
8. Marone, A.; Carmona-Martínez, A.A.; Sire, Y.; Meudec, E.; Steyer, J.P.; Bernet, N.; Trably, E. Bioelectrochemical treatment of table olive brine processing wastewater for biogas production and phenolic compounds removal. *Water Res.* **2016**, *100*, 316–325. [[CrossRef](#)] [[PubMed](#)]
9. Zubchenko, L.; Kuzminskiy, Y. Characteristics of biofilm formation process in the bioelectrochemical systems, working in batch-mode of cultivation. *Chem. Chem. Technol.* **2017**, *11*, 105–110. [[CrossRef](#)]

10. Kouzuma, A.; Ishii, S.; Watanabe, K. Metagenomic insights into the ecology and physiology of microbes in bioelectrochemical systems. *Bioresour. Technol.* **2018**, *255*, 302–307. [[CrossRef](#)]
11. Nijenhuis, I.; Nikolausz, M.; Köth, A.; Felföldi, T.; Weiss, H.; Drangmeister, J.; Großmann, J.; Kästner, M.; Richnow, H.H. Assessment of the natural attenuation of chlorinated ethenes in an anaerobic contaminated aquifer in the Bitterfeld/Wolfen area using stable isotope techniques, microcosm studies and molecular biomarkers. *Chemosphere* **2007**, *67*, 300–311. [[CrossRef](#)]
12. Dowideit, K.; Scholz-Muramatsu, H.; Miethling-Graff, R.; Vigelahn, L.; Freygang, M.; Dohrmann, A.B.; Tebbe, C.C. Spatial heterogeneity of dechlorinating bacteria and limiting factors for in situ trichloroethene dechlorination revealed by analyses of sediment cores from a polluted field site. *FEMS Microbiol. Ecol.* **2010**, *71*, 444–459. [[CrossRef](#)]
13. Chang, Y.H.; Cheng, T.W.; Lai, W.J.; Tsai, W.Y.; Sun, C.H.; Lin, L.H.; Wang, P.L. Microbial methane cycling in a terrestrial mud volcano in eastern Taiwan. *Environ. Microbiol.* **2012**, *14*, 895–908. [[CrossRef](#)]
14. Pfennig, N.; Biebl, H. *Desulfuromonas acetoxidans* gen. nov. and sp. nov., a new anaerobic, sulfur-reducing, acetate-oxidizing bacterium. *Arch. Microbiol.* **1976**. [[CrossRef](#)] [[PubMed](#)]
15. Finster, K.; Bak, F.; Pfennig, N. *Desulfuromonas acetexigens* sp. nov., a dissimilatory sulfur-reducing eubacterium from anoxic freshwater sediments. *Arch. Microbiol.* **1994**. [[CrossRef](#)]
16. Coates, J.D.; Lonergan, D.J.; Philips, E.J.P.; Jenter, H.; Lovley, D.R.; Lovley, D.R. *Desulfuromonas palmitatis* sp. nov., a marine dissimilatory Fe(III) reducer that can oxidize long-chain fatty acids. *Arch. Microbiol.* **1995**, *164*, 406–413. [[CrossRef](#)] [[PubMed](#)]
17. Finster, K.; Coates, J.D.; Liesack, W.; Pfennig, N. *Desulfuromonas thiophila* sp. nov., a new obligately sulfur-reducing bacterium from anoxic freshwater sediment. *Int. J. Syst. Bacteriol.* **1997**, *47*, 754–758. [[CrossRef](#)] [[PubMed](#)]
18. Krumholz, L.R. *Desulfuromonas chloroethenica* sp. nov. uses tetrachloroethylene and trichloroethylene as electron acceptors. *Int. J. Syst. Bacteriol.* **1997**, *47*, 1262–1263. [[CrossRef](#)]
19. Sung, Y.; Ritalahti, K.M.; Sanford, R.A.; Urbance, J.W.; Flynn, S.J.; Tiedje, J.M.; Löffler, F.E. Characterization of two tetrachloroethene-reducing, acetate-oxidizing anaerobic bacteria and their description as *Desulfuromonas michiganensis* sp. nov. *Appl. Environ. Microbiol.* **2003**, *69*, 2964–2974. [[CrossRef](#)] [[PubMed](#)]
20. Vandieken, V.; Mußmann, M.; Niemann, H.; Jørgensen, B.B. *Desulfuromonas svalbardensis* sp. nov. and *Desulfuromusa ferrireducens* sp. nov., psychrophilic, Fe(III)-reducing bacteria isolated from Arctic sediments, Svalbard. *Int. J. Syst. Evol. Microbiol.* **2006**, *56*, 1133–1139. [[CrossRef](#)]
21. An, T.T.; Picardal, F.W. *Desulfuromonas carbonis* sp. nov., an Fe(III)-, S₀- and Mn(IV)-reducing bacterium isolated from an active coalbed methane gas well. *Int. J. Syst. Evol. Microbiol.* **2015**, *65*, 1686–1693. [[CrossRef](#)]
22. Kim, S.; Park, S.; Cha, I.; Min, D.; Kim, J.; Chung, W.; Chae, J.; Jeon, C.O.; Rhee, S. Metabolic versatility of toluene-degrading, iron-reducing bacteria in tidal flat sediment, characterized by stable isotope probing-based metagenomic analysis. *Environ. Microbiol.* **2014**, *16*, 189–204. [[CrossRef](#)]
23. Guo, Y.; Aoyagi, T.; Inaba, T.; Sato, Y.; Habe, T.H.H. Complete Genome Sequence of *Desulfuromonas* sp. Strain AOP6, an Iron (III) Reducer Isolated from Subseafloor Sediment. *Microbiol. Resour. Announc.* **2020**, *9*, e01325-19. [[CrossRef](#)] [[PubMed](#)]
24. Zhang, T.; Bain, T.S.; Barlett, M.A.; Dar, S.A.; Snoeyenbos-West, O.L.; Nevin, K.P.; Lovley, D.R. Sulfur oxidation to sulfate coupled with electron transfer to electrodes by *Desulfuromonas* strain TZ1. *Microbiology* **2014**, *160*, 123–129. [[CrossRef](#)] [[PubMed](#)]
25. Badalamenti, J.P.; Summers, Z.M.; Chan, C.H.; Gralnick, J.A.; Bond, D.R. Isolation and genomic characterization of “*Desulfuromonas soudanensis* WTL”, a metal- and electrode-respiring bacterium from anoxic deep subsurface brine. *Front. Microbiol.* **2016**, *7*, 1–11. [[CrossRef](#)] [[PubMed](#)]
26. Jacobsen, T.; Bardiaux, B.; Francetic, O.; Izadi-Pruneyre, N.; Nilges, M. Structure and function of minor pilins of type IV pili. *Med. Microbiol. Immunol.* **2020**, *209*, 301–308. [[CrossRef](#)] [[PubMed](#)]
27. Yoshida, N.; Goto, Y.; Miyata, Y.; Thakur, V.K. Selective growth of and electricity production by marine exoelectrogenic bacteria in self-aggregated hydrogel of microbially reduced graphene oxide. *C. J. Carbon Res.* **2016**, *2016*, 15. [[CrossRef](#)]
28. Yoshida, N.; Miyata, Y.; Doi, K.; Goto, Y.; Nagao, Y.; Tero, R.; Hiraishi, A. Graphene oxide-dependent growth and self-Aggregation into a hydrogel complex of exoelectrogenic bacteria. *Sci. Rep.* **2016**, *6*, 15. [[CrossRef](#)]
29. Goto, Y.; Yoshida, N.; Umeyama, Y.; Yamada, T.; Tero, R.; Hiraishi, A. Enhancement of electricity production by graphene oxide in soil microbial fuel cells and plant microbial fuel cells. *Front. Bioeng. Biotechnol.* **2015**, *3*, 42. [[CrossRef](#)] [[PubMed](#)]
30. Goto, Y.; Yoshida, N. Scaling up microbial fuel cells for treating. *Water* **2019**, *11*, 1803. [[CrossRef](#)]
31. Goto, Y.; Yoshida, N. Microbially reduced graphene oxide shows efficient electricity recovery from artificial dialysis wastewater. *J. Gen. Appl. Microbiol.* **2017**, *63*, 165–171. [[CrossRef](#)]
32. Yoshida, N.; Miyata, Y.; Mugita, A.; Iida, K. Electricity recovery from municipal sewage wastewater using a hydrogel complex composed of microbially reduced graphene oxide and sludge. *Materials* **2016**, *9*, 742. [[CrossRef](#)] [[PubMed](#)]
33. Yoshida, N.; Asahi, K.; Sakakibara, Y.; Miyake, K.; Katayama, A. Isolation and quantitative detection of tetrachloroethene (PCE)-dechlorinating bacteria in unsaturated subsurface soils contaminated with chloroethenes. *J. Biosci. Bioeng.* **2007**, *104*, 91–97. [[CrossRef](#)] [[PubMed](#)]
34. Ismaeil, M.; Yoshida, N.; Katayama, A. *Bacteroides sedimenti* sp. nov., isolated from a chloroethenes-dechlorinating consortium enriched from river sediment. *J. Microbiol.* **2018**, *56*, 619–627. [[CrossRef](#)] [[PubMed](#)]
35. Nagahashi, W.; Yoshida, N. Comparative evaluation of fibrous artificial carbons and bamboo charcoal in terms of recovery of current from sewage wastewater. *J. Gen. Appl. Microbiol.* **2021**, in press. [[CrossRef](#)]

36. Tamaoka, J.; Katayama-Fujimura, Y.; Kuraishi, H. Analysis of bacterial menaquinone mixtures by high performance liquid chromatography. *J. Appl. Bacteriol.* **1983**, *54*, 31–36. [[CrossRef](#)]
37. Ismaeil, M.; Yoshida, N.; Katayama, A. Identification of multiple dehalogenase genes involved in tetrachloroethene-to-ethene dechlorination in a dehalococoides-dominated enrichment culture. *Biomed. Res. Int.* **2017**, *2017*, 9191086. [[CrossRef](#)] [[PubMed](#)]
38. Tanizawa, Y.; Fujisawa, T.; Nakamura, Y. DFAST: A flexible prokaryotic genome annotation pipeline for faster genome publication. *Bioinformatics* **2018**, *34*, 1037–1039. [[CrossRef](#)]
39. Overbeek, R.; Olson, R.; Pusch, G.D.; Olsen, G.J.; Davis, J.J.; Disz, T.; Edwards, R.A.; Gerdes, S.; Parrello, B.; Shukla, M.; et al. The SEED and the rapid annotation of microbial genomes using Subsystems Technology (RAST). *Nucleic Acids Res.* **2014**, *42*, 206–214. [[CrossRef](#)]
40. Kumar, S.; Stecher, G.; Li, M.; Niyaz, C.; Tamura, K. MEGA X: Molecular evolutionary genetics analysis across computing platforms. *Mol. Biol. Evol.* **2018**, *35*, 1547–1549. [[CrossRef](#)] [[PubMed](#)]
41. Meier-Kolthoff, J.P.; Göker, M.; Spröer, C.; Klenk, H.P. When should a DDH experiment be mandatory in microbial taxonomy? *Arch. Microbiol.* **2013**, *195*, 413–418. [[CrossRef](#)]
42. Kim, M.; Oh, H.S.; Park, S.C.; Chun, J. Towards a taxonomic coherence between average nucleotide identity and 16S rRNA gene sequence similarity for species demarcation of prokaryotes. *Int. J. Syst. Evol. Microbiol.* **2014**, *64*, 346–351. [[CrossRef](#)] [[PubMed](#)]
43. Sun, D.; Wang, A.; Cheng, S.; Yates, M.; Logan, B.E. *Geobacter anodireducens* sp. nov., an exoelectrogenic microbe in bioelectrochemical systems. *Int. J. Syst. Evol. Microbiol.* **2014**, *64*, 3485–3491. [[CrossRef](#)] [[PubMed](#)]
44. Viulu, S.; Nakamura, K.; Okada, Y.; Saitou, S.; Takamizawa, K. *Geobacter luticola* sp. nov., an Fe(III)-reducing bacterium isolated from lotus field mud. *Int. J. Syst. Evol. Microbiol.* **2013**, *63*, 442–448. [[CrossRef](#)]
45. Shelobolina, E.S.; Vronis, H.A.; Findlay, R.H.; Lovley, D.R. *Geobacter uraniireducens* sp. nov., isolated from subsurface sediment undergoing uranium bioremediation. *Int. J. Syst. Evol. Microbiol.* **2008**, *58*, 1075–1078. [[CrossRef](#)] [[PubMed](#)]
46. Shelobolina, E.S.; Nevin, K.P.; Blakeney-Hayward, J.D.; Johnsen, C.V.; Plaia, T.W.; Krader, P.; Woodard, T.; Holmes, D.E.; VanPraagh, C.G.; Lovley, D.R. *Geobacter pickeringii* sp. nov., *Geobacter argillaceus* sp. nov. and *Pelosinus fermentans* gen. nov., sp. nov., isolated from subsurface kaolin lenses. *Int. J. Syst. Evol. Microbiol.* **2007**, *57*, 126–135. [[CrossRef](#)]
47. Hedrick, D.B.; Peacock, A.D.; Lovley, D.R.; Woodard, T.L.; Nevin, K.P.; Long, P.E.; White, D.C. Polar lipid fatty acids, LPS-hydroxy fatty acids, and respiratory quinones of three *Geobacter* strains, and variation with electron acceptor. *J. Ind. Microbiol. Biotechnol.* **2009**, *36*, 205–209. [[CrossRef](#)] [[PubMed](#)]
48. Kunapuli, U.; Jahn, M.K.; Lueders, T.; Geyer, R.; Heipieper, H.J.; Meckenstock, R.U. *Desulfitobacterium aromaticivorans* sp. nov. and *Geobacter toluenoxidans* sp. nov., iron-reducing bacteria capable of anaerobic degradation of monoaromatic hydrocarbons. *Int. J. Syst. Evol. Microbiol.* **2010**, *60*, 686–695. [[CrossRef](#)]
49. Chen, C.; Chen, H.; Zhang, Y.; Thomas, H.R.; Frank, M.H.; He, Y. TBtools: An integrative toolkit developed for interactive analyses of big biological data. *Mol. Plant.* **2020**, *13*, 1194–1202. [[CrossRef](#)]
50. Sigrist, C.J.A.; Cerutti, L.; Hulo, N.; Gattiker, A.; Falquet, L.; Pagni, M.; Bairoch, A.; Bucher, P. PROSITE: A documented database using patterns and profiles as motif descriptors. *Brief. Bioinform.* **2002**, *3*, 265–274. [[CrossRef](#)]
51. Jiang, Y.; Shi, M.; Shi, L. Molecular underpinnings for microbial extracellular electron transfer during biogeochemical cycling of earth elements. *Sci. China Life Sci.* **2019**, *62*, 1275–1286. [[CrossRef](#)] [[PubMed](#)]
52. Levar, C.E.; Chan, C.H.; Mehta-Kolte, M.G.; Bond, D.R. An inner membrane cytochrome required only for reduction of high redox potential extracellular electron acceptors. *MBio* **2014**, *5*, e02034-14. [[CrossRef](#)]
53. Levar, C.E.; Hoffman, C.L.; Dunshee, A.J.; Toner, B.M.; Bond, D.R. Redox potential as a master variable controlling pathways of metal reduction by *Geobacter sulfurreducens*. *ISME J.* **2017**, *11*, 741–752. [[CrossRef](#)]
54. Morgado, L.; Brulx, M.; Pessanha, M.; Londer, Y.Y.; Salgueiro, C.A. Thermodynamic characterization of a triheme cytochrome family from *geobacter sulfurreducens* reveals mechanistic and functional diversity. *Biophys. J.* **2010**, *99*, 293–301. [[CrossRef](#)] [[PubMed](#)]
55. Liu, Y.; Fredrickson, J.K.; Zachara, J.M.; Shi, L. Direct involvement of ombB, omaB, and omcB genes in extracellular reduction of Fe (III) by *Geobacter sulfurreducens* PCA. *Front. Microbiol.* **2015**, *6*, 1075. [[CrossRef](#)]
56. Liu, Y.; Wang, Z.; Liu, J.; Levar, C.; Edwards, M.J.; Babauta, J.T.; Kennedy, D.W.; Shi, Z.; Beyenal, H.; Bond, D.R.; et al. A trans-outer membrane porin-cytochrome protein complex for extracellular electron transfer by *Geobacter sulfurreducens* PCA. *Environ. Microbiol. Rep.* **2014**, *6*, 776–785. [[CrossRef](#)] [[PubMed](#)]
57. Otero, F.J.; Chan, C.H.; Bond, D.R. Identification of different putative outer membrane electron conduits necessary for Fe(III) citrate, Fe(III) oxide, Mn(IV) oxide, or electrode reduction by *Geobacter sulfurreducens*. *J. Bacteriol.* **2018**, *200*, e00347-18. [[CrossRef](#)]
58. Trumpower, B. The protonmotive Q cycle. *J. Biol. Chem.* **1990**, *265*, 11409–11412. [[CrossRef](#)]
59. Mollaei, M.; Timmers, P.H.A.; Suarez-Diez, M.; Boeren, S.; van Gelder, A.H.; Stams, A.J.M.; Plugge, C.M. Comparative proteomics of *Geobacter sulfurreducens* PCAT in response to acetate, formate and/or hydrogen as electron donor. *Environ. Microbiol.* **2021**, *23*, 299–315. [[CrossRef](#)]
60. Seidel, J.; Hoffmann, M.; Ellis, K.E.; Seidel, A.; Spatzal, T.; Gerhardt, S.; Elliott, S.J.; Einsle, O. MacA is a second cytochrome c peroxidase of *Geobacter sulfurreducens*. *Biochemistry* **2012**, *51*, 2747–2756. [[CrossRef](#)]
61. Aklujkar, M.; Coppi, M.V.; Leang, C.; Kim, B.C.; Chavan, M.A.; Perpetua, L.A.; Giloteaux, L.; Liu, A.; Holmes, D.E. Proteins involved in electron transfer to Fe (III) and Mn (IV) oxides by *Geobacter sulfurreducens* and *Geobacter uraniireducens*. *Microbiology* **2013**, *159*, 515–535. [[CrossRef](#)]

62. Butler, J.E.; Young, N.D.; Lovley, D.R. Evolution of electron transfer out of the cell: Comparative genomics of six *Geobacter* genomes. *BMC Genom.* **2010**, *11*, 40. [[CrossRef](#)]
63. Zheng, S.; Liu, F.; Li, M.; Xiao, L.; Wang, O. Comparative transcriptomic insights into the mechanisms of electron transfer in *Geobacter* co-cultures with activated carbon and magnetite. *Sci. China Life Sci.* **2018**, *61*, 787–798. [[CrossRef](#)] [[PubMed](#)]
64. Craig, L.; Forest, K.T.; Maier, B. Type IV pili: Dynamics, biophysics and functional consequences. *Nat. Rev. Microbiol.* **2019**, *17*, 429–440. [[CrossRef](#)] [[PubMed](#)]
65. Lovley, D.R.; Walker, D.J.F. *Geobacter* protein nanowires. *Front. Microbiol.* **2019**, *10*, 2078. [[CrossRef](#)]
66. Lovley, D.R. Electrically conductive pili: Biological function and potential applications in electronics. *Curr. Opin. Electrochem.* **2017**, *4*, 190–198. [[CrossRef](#)]
67. Walker, D.J.; Adhikari, R.Y.; Holmes, D.E.; Ward, J.E.; Woodard, T.L.; Nevin, K.P.; Lovley, D.R. Electrically conductive pili from pilin genes of phylogenetically diverse microorganisms. *ISME J.* **2018**, *12*, 48–58. [[CrossRef](#)]
68. Herzberg, M.; Kaye, I.K.; Peti, W.; Wood, T.K. YdgG (TqsA) controls biofilm formation in *Escherichia coli* K-12 through autoinducer 2 transport. *J. Bacteriol.* **2006**, *188*, 587–598. [[CrossRef](#)]
69. Button, J.E.; Silhavy, T.J.; Ruiz, N. A suppressor of cell death caused by the loss of σ^E downregulates extracytoplasmic stress responses and outer membrane vesicle production in *Escherichia coli*. *J. Bacteriol.* **2007**, *189*, 1523–1530. [[CrossRef](#)]